

[Click here to view linked References](#)

1  
2  
3  
4  
5  
6  
7  
8  
9  
10  
11  
12  
13  
14  
15  
16  
17  
18  
19  
20  
21  
22  
23  
24  
25  
26  
27  
28  
29  
30  
31  
32  
33  
34  
35  
36  
37  
38  
39  
40  
41  
42  
43  
44  
45  
46  
47  
48  
49  
50  
51  
52  
53  
54  
55  
56  
57  
58  
59  
60  
61  
62  
63  
64  
65

# Removal of Macro-pollutants in Oily Wastewater Obtained from Soil Remediation Plant Using Electro-oxidation Process

Mehdi Zolfaghari <sup>a</sup>, Patrick Drogui <sup>a\*</sup>, Jean François Blais <sup>a</sup>

<sup>a</sup> Institut National de la Recherche Scientifique, Eau, Terre et Environnement (INRS-ETE),  
Université du Québec, 490 rue de la Couronne, Québec, QC, Canada, G1K 9A9.

\* Corresponding author

Author email: mehdi.zolfaghari@ete.inrs.ca

patrick.drogui@ete.inrs.ca

jean-francois.blais@inrs.ca

September 2017

## Abstract

Electro-oxidation process by Niobium boron-doped diamond (Nb/BDD) electrode was used to treat non-biodegradable oily wastewater provided from soil leachate contaminated by hydrocarbons. Firstly, the diffusion current limit and mass transfer coefficient was experimentally measured ( $7.1 \text{ mA cm}^{-2}$  and  $14.7 \text{ } \mu\text{m s}^{-1}$ , respectively), in order to understand minimum applied current density. Later on, the oxidation kinetic model of each pollutant was investigated in different current densities ranged between 3.8 to  $61.5 \text{ mA cm}^{-2}$ . It was observed that direct oxidation was the main removal mechanism of organic and inorganic carbon; while, the indirect oxidation in higher current density was responsible for nitrogen oxidation. Hydrocarbon in the form of colloidal particles could be removed by electro-flotation. On the other hand, electro-decomposition on the surface of cathode and precipitation by hydroxyl ions were the utmost removal pathway of metals. According to the initial experiments, operating condition was further optimized by central composite design model in different current density, treatment time, and electrolyte addition, based on the best responses on the specific energy consumption (SEC), chemical oxygen demand (COD) and total organic carbon (TOC) removal efficiency. Under optimum operating condition (current density =  $23.1 \text{ mA cm}^{-2}$ , time = 120 min, Ti/Pt as a cathode and Nb/BDD as the anode), electro-oxidation showed the following removal efficiencies: COD (84.6%), TOC (68.2%), oil and grease (99%), Color (87.9%), total alkalinity (92%),  $N_{\text{tot}}$  (18%),  $\text{NH}_4^+$  (31%), Ca (66.4%), Fe (71.1%), Mg (41.4%), Mn (78.1%),  $P_{\text{tot}}$  (75%), S (67.1%), and Si (19.1%).

## Keywords:

Oily wastewater; Electro-oxidation process; Oxidation kinetics; Optimization.

1  
2  
3  
4 **Nomenclature**  
5  
6

7  
8 BDD Boron-doped diamond  
9  
10 BOD Biochemical Oxygen Demand  
11  
12 CCD Central Composite Design  
13  
14 CD Current Density  
15  
16 COD Chemical Oxygen Demand  
17  
18  
19  $I_{lim}$  Diffusion Current Limit  
20  
21 EC Electrical Conductivity  
22  
23  
24 FD Factorial Design  
25  
26  $\eta$  Instant Current Efficiency  
27  
28  
29 OWW Oily Wastewater  
30  
31 SEC Specific Energy Consumption  
32  
33  
34 TA Total Alkalinity  
35  
36 TCU True Color Unit  
37  
38 TOC Total Organic Carbon  
39  
40  
41  
42  
43  
44  
45  
46  
47  
48  
49  
50  
51  
52  
53  
54  
55  
56  
57  
58  
59  
60  
61  
62  
63  
64  
65

# 1 Introduction

Produced water from the petroleum refinery, oil storage and transportation, petrochemical industry, oil-drilling mud and oily contaminated soil leachate are categorized as the oily wastewater (OWW) (Yu et al. 2017). These wastewaters mostly contains high concentration of hydrocarbons, phenols, sulfides, heavy metals and ammonia (NH<sub>3</sub>) with very high toxicity (Skban Ibrahim et al. 2014). Although utilization of specific strains of microorganism could potentially remove prevalent hydrocarbon compounds (Tazari et al. 2017), lack of biodegradable organic carbon and phosphorous brings challenges for the biological treatment processes (Yu et al. 2017). Additionally, physical separation such as, API oil-water separator and dissolved air flotation has deficiency for proper removal of fine colloids hydrocarbon with diameter of 0.1-100 µm (Al-Shamrani et al. 2002, Santos et al. 2006).

Simplicity of process, ease of operation, minimal sludge production, brief retention time and high performance in the oxidation of macro and micro-pollutants makes electro-oxidation process one of the best treatment option ~~for treatment~~ of non-biodegradable industrial wastewater such as, oily wastewater, landfill leachate, textile dye, pulp and paper and aquaculture saline water (Bashir et al. 2013, da Silva et al. 2013, Díaz et al. 2011, Drogui et al. 2007, Zolfaghari et al. 2016). Electro-oxidation used not only used for low quantity wastewater with high electrical conductivity (EC), but also ~~it used asfor~~ treatment of light wastewater with COD below 800 mg L<sup>-1</sup> (da Silva et al. 2013) or as the post treatment of municipal wastewater treatment plant with low energy consumption (4.3 kWh m<sup>-3</sup>) (Cao et al. 2016). In this case, energy consumption could be cut off by the addition of salt such as NaCl and Na<sub>2</sub>SO<sub>4</sub> (Chen 2004, Díaz et al. 2011, Panizza & Martinez-Huitle 2013).

1  
2  
3  
4 Basically anode materials are made up special composites that produce hydroxyl radicals ( $\text{OH}^\circ$ )  
5 instead of oxygen (Yavuz et al. 2010). Anodic pollutants oxidation on the surface of electrode  
6 and in the interface by  $\text{OH}^\circ$  was called direct oxidation (Anglada et al. 2011, Bashir et al. 2013,  
7 Cao et al. 2016). In higher current density (CD) ions and water molecule are electrochemically  
8 react with  $\text{OH}^\circ$  or directly on the surface of anode to generate mediator radicals, such as  
9 hypochlorous acid ( $\text{HClO}$ ), peroxydisulfuric acid ( $\text{H}_2\text{S}_2\text{O}_8$ ), hydrogen peroxide ( $\text{H}_2\text{O}_2$ ), and  
10 ozone ( $\text{O}_3$ )~~that oxidized the pollutants~~. The only removal pathway of  $\text{NH}_4^+$  was through indirect  
11 oxidation by  $\text{HClO}$  (Díaz et al. 2011, Ighilahriz et al. 2013, Li & Liu 2009).  
12  
13

14  
15  
16 Compare to the other mixed metal oxide electrodes (da Silva et al. 2013), non-active BDD  
17 ~~electrode has~~shows the highest performance on hydroxyl radical generation (Zhou et al. 2016);  
18 ~~as it shows~~due to low adsorption enthalpy of  $\text{OH}^\circ$  (Martínez-Huitile & Brillas 2008). For example,  
19 ~~the reaction rate of~~phenol and COD oxidation rate using BDD was 12 times higher than Ru-  
20 MMO electrode, even though the current density was four times smaller (Yavuz et al. 2010).  
21  
22  
23

24  
25  
26 In this study, the oxidation mechanisms of all macro-contaminants were firstly investigated by  
27 focusing on their kinetic studies. Later on, the effect of operating conditions was investigated on  
28 the process performance. Finally, the operating condition was optimized according to the best  
29 oxidation performance and energy consumption.  
30  
31  
32  
33  
34  
35  
36  
37  
38  
39  
40  
41  
42  
43  
44  
45  
46  
47  
48  
49  
50  
51  
52  
53  
54  
55  
56  
57  
58  
59  
60  
61  
62  
63  
64  
65

## 2 Material and Methods

### 2.1 Oily wastewater

OWW was taken from the leachate of soil remediation plant, located in 5 km North of Quebec City, QC, Canada. The treatment plant received soil from the nearby site, which was heavily contaminated by crude petroleum. Prior to release into the environment, the soil leachate introduced to a primary settling tank for suspended solid (~~SS~~) removal, followed by peat filtration for the adsorption of humic substances and granular activated carbon for the removal of recalcitrant hydrocarbon. In 10<sup>th</sup> of May 2016, 60 liters of sample was taken directly from primary settling tank, instantly keeping in cold room with temperature of 4°C, before the experiments. According to the characteristic of OWW presented in Table 1, the current treatment facility should be modified to remove effectively residual NH<sub>3</sub>, metals and total organic carbon (TOC). Deficiency of biological treatment was inevitable, due to the low ratio of BOD/COD and lack of phosphorous. Deposition of suspended solidSS on the surface of electrodes negatively influences the oxidation by increasing the electrical resistance; yet, its concentration was insignificant after the primary settling tank.

### 2.2 Experimental pilot

The electrochemical oxidation pilot was made up two Plexiglas containers in close loop: (1) reaction tank with dimension of (14 × 5 × 10 cm), (2) and a 500 mL storage tank. The rectangular anode/cathode electrode made up niobium coated with 4 μm of boron doped diamond (Nb/BDD) (provided by DiaChem®, Germany) and titanium coated with platinum (Ti/Pt) with the thickness of 0.1 cm, specific surface area of 130 cm<sup>2</sup> and inter-electrode gap of 1 cm ~~were used~~. Coating of BDD on the surface of Nb was performed by hot filament chemical

1  
2  
3  
4 vapor deposition in presence of  $\text{KFe}(\text{CN})_6$  under acidic condition. Niobium was also selected as  
5  
6 the base metal, due to its high corrosion resistance, working in high temperature and high  
7  
8 adhesion capability (Yu et al. 2013). Furthermore, BDD coating showed ~~Nb/BDD was selected,~~  
9  
10 ~~because of high corrosive resistance,~~ low hydroxyl radical adsorption properties, stable chemical  
11  
12 properties and high catalytic activity (Chen 2004, Panizza et al. 2001). Stability of BDD coating  
13  
14 was proved in this study, as the concentration of Boron was changed insignificantly during all  
15  
16 sets of experiment (Table 1). Likewise, Ti/Pt was selected as the cathode type, due to its  
17  
18 resistance toward nitrate reduction into ammonia (Ding et al. 2015). The electric current was  
19  
20 provided by a DC power supply (Sorensen DCS40-75E, Magna-Power Electronics Inc.,  
21  
22 Flemington, New Jersey, USA). In order to maximized the mass transfer rate, the recycling flow  
23  
24 rate was kept around  $190 \text{ mL min}^{-1}$  by a peristaltic pump (Masterflex L/S, Cole-Parmer Co.,  
25  
26 Montreal, QC, Canada) (Skban Ibrahim et al. 2014). Due to the metal electrodeposition and/or  
27  
28 precipitation on the surface of cathode, ~~it~~ the electrodes submerged in the solution of 5%  
29  
30 hydrochloric acid for 30 min after each experiment.  
31  
32  
33  
34  
35  
36  
37  
38  
39  
40  
41

### 42 **2.3 Experimental design**

43  
44 Kinetic studies were performed in different current density from  $3.8$  to  $61.5 \text{ mA cm}^{-2}$ , in order to  
45  
46 calculate the diffusion current limit ( $I_{\text{lim}}$ ), mechanism of macro-pollutant oxidation and proper  
47  
48 range of operating condition. Two main operating regimes control the oxidation of organic  
49  
50 matter: (1) electronic transfer control; and (2) mass transport control (Panizza & Martinez-Huitle  
51  
52 2013). In low current density, electronic transfer controlled the oxidation rate, resulted in zero-  
53  
54 order kinetics of COD oxidation. If COD oxidation followed first-order kinetic, oxidation was  
55  
56 mainly controlled by mass transfer. By knowing the fact that instant current efficiency ( $\eta$ )  
57  
58  
59  
60  
61  
62  
63  
64  
65

1  
2  
3  
4 decreases below 1 for current density larger than  $I_{lim}$  (equation 1), it gradually decreased to reach  
5  
6  $\eta = 1$ . Kinetics of COD oxidation in  $I_{lim}$  was used for experimental estimation of  $K_m$ , based on  
7  
8  
9 equation 2:

$$\eta = \frac{4FV_R(COD_t - COD_0)}{It} \quad (1)$$

$$I_{lim} = 4FAK_m COD(t) = 4FAK_m COD_0 \exp(-kt) \quad (2)$$

10  
11  
12  
13  
14  
15  
16  
17  
18  
19  
20  
21  
22  
23  
24  
25 Where, F stands for Faraday's constant (96,487 C mol<sup>-1</sup>), COD<sub>0</sub> and COD<sub>t</sub> are initial and final  
26  
27 concentration (mol. L<sup>-1</sup>), t is the time of reaction, A is the surface of anode (m<sup>2</sup>), and V<sub>R</sub> is the  
28  
29 volume of wastewater (L) (Boye et al. 2004).  
30  
31

32  
33 The kinetic study was performed by measuring the residual COD, TOC, N<sub>tot</sub>, NO<sub>3</sub><sup>-</sup> and NH<sub>4</sub><sup>+</sup> for  
34  
35 each sample taken in specific period of time (5, 10, 20, 30, 45, 60, 90, 120 min). Na<sub>2</sub>SO<sub>4</sub> with  
36  
37 concentration of 1 g L<sup>-1</sup> was inserted to increase the electrical conductivity from the average 2.75  
38  
39 to 4.89 ms cm<sup>-1</sup>. The addition of electrolyte decreased the applied electric potential, consequently  
40  
41 decreased the energy consumption.  
42  
43  
44

45  
46 For understanding the statistical significance of variable parameters such as, current density (X<sub>1</sub>),  
47  
48 treatment time (X<sub>2</sub>) and addition of electrolyte (X<sub>3</sub>), factorial design (FD) was used with specific  
49  
50 energy consumption, COD and TOC removal efficiency as the responses. The condition of FD  
51  
52 experiments was fixed in extreme limit with eight sets of experiments. Additional eighteen sets  
53  
54 of experiments at the center of domain and axial assays for each categorical factor were  
55  
56 performed for process optimization by central composite design (CCD). All the conditions and  
57  
58 results of FD and CCD models were provided in Table 2.  
59  
60  
61

1  
2  
3  
4 In FD, the effect of each factor and their interaction was estimated according to the following  
5  
6 model (Equation 3):  
7  
8  
9

$$Y = b_0 + b_1X_1 + b_2X_2 + b_3X_3 + b_{12}X_{12} + b_{13}X_{13} + b_{23}X_{23} \quad (3)$$

10  
11  
12  
13  
14  
15  
16  
17  
18 In which Y is the experimental response,  $b_0$  is the average value of response,  $X_i$  is the variables,  
19  
20  $b_i$  stands for effect of each factor and finally  $b_{ij}$  represents interaction effect of variable i and j on  
21  
22 response. Experimental coefficient (b) was measured using half difference between arithmetic  
23  
24 averages of the responses for extreme values of variable. For the process optimization, CCD  
25  
26 model was performed by means of 26 experiments, ~~and which later~~ estimated the result by  
27  
28 second order model ~~(Equation 4)~~.  
29  
30  
31  
32  
33  
34  
35  
36

$$Y = b_0 + \sum b_i X_i + \sum b_{ii} X_i^2 + \sum b_{ij} X_i X_j + e_i \quad (4)$$

37  
38  
39  
40  
41  
42 In ~~which equation 4~~,  $b_i$ ,  $b_{ii}$  and  $b_{ij}$  are the liner, quadratic and interactive effects of specified  
43  
44 variable and  $e_i$  represents the residual term. Design expert software (Design Expert 7, State-Ease  
45  
46 Inc., Minneapolis, USA) was used to calculate the coefficients of polynomial model.  
47  
48  
49

50  
51 The specific energy consumption ( $\text{kWh kg COD}^{-1}$ ) was calculated according to the following  
52  
53 equation:  
54  
55  
56  
57

$$SEC = \frac{I \Delta U t}{V_R (COD_t - COD_0)} \quad (5)$$

1  
2  
3  
4  
5  
6  
7 Where I stand for current intensity (A),  $\Delta U$  is the average cell voltage (V), t is the treatment time  
8  
9 (h), and COD unit is  $\text{g L}^{-1}$  (Skban Ibrahim et al. 2014).  
10  
11  
12  
13  
14

#### 15 **2.4 Sampling and analysis**

16  
17

18 Samples from electro-oxidation reactor were kept frozen at  $-18^{\circ}\text{C}$ , prior to analysis. COD and  
19 color was measured by spectrophotometer (Cary 50, Varian Canada Inc., Mississauga, ON,  
20 Canada). TOC and  $N_{\text{tot}}$  were analyzed using a Shimadzu TOC 5000A/ TNM-L analyzer  
21 (Shimadzu Co., Laval, Qc, Canada). Lachat Instrument was used for analyzing ammonium  
22 ( $\text{NH}_4^+$ ), nitrite ( $\text{NO}_2^-$ ), nitrate ( $\text{NO}_3^-$ ) and ortho-phosphate ( $\text{PO}_4^{3-}$ ) assimilated by QuikChem  
23 method 10-107-06-2-B, 10-107-4-2-A and 10-115-01-1-B, respectively. Total alkalinity (TA)  
24 was analyzed based on colorimetric titration with 0.02 N of sulfuric acid solution in the presence  
25 of methyl orange. Around 15 mL of each sample was digested by 3 mL of hydrogen peroxide in  
26 the presence of 2 mL of nitric acid before inserting into the ICP/MS for the metal analysis. The  
27 procedure of extraction and analysis of metal are fully describe in previous studies\_(Zolfaghari et  
28 al. 2016).  
29  
30  
31  
32  
33  
34  
35  
36  
37  
38  
39  
40  
41  
42  
43  
44  
45  
46  
47  
48  
49  
50  
51  
52  
53  
54  
55  
56  
57  
58  
59  
60  
61  
62  
63  
64  
65

### 3 Results and Discussion

#### 3.1 Estimation of limiting current density

While working under galvanostatic conditions, it can be possible to identify two different operating regimes; i) electronic transfer control and ii) mass transport control.  $I_{lim}$  is the current intensity for which the rate of pollutant removal is maximal (Equation 2). When the electrolysis is under current control ( $I < I_{lim}$ ), the instantaneous current efficiency is equal to 100% and COD removal rate of COD removal is constant. However, when the electrolysis is under mass transport control ( $I > I_{lim}$ ), the applied current density exceed the limiting- current density- and secondary reactions (such as oxygen evolution) takes place, resulting in a decrease of the instantaneous current efficiency ( $\eta$ ). Energy consumption is the most decisive factor in the selection of advanced oxidation processes. Increasing the efficiency of the process is the main objective that measured by gradual increase of current density. Experimental calculation of  $I_{lim}$  and  $K_m$  requires calculation of  $\eta$  in different range of current density. According to the results presented in Figure 1, the limited current density occurred at  $6.2 \text{ mA cm}^{-2}$ , as the  $\eta$  was becoming so close to 100%. By considering the homogenous first-order kinetic constant rate in  $I_{lim}$  (Equation 2), the calculated value of  $K_m$  was around  $14.7 \text{ } \mu\text{m s}^{-1}$  ~~which-that~~ was close to the value of 10 (Körbahti & Artut 2010), 17.5 (Anglada et al. 2011) and  $30 \text{ } \mu\text{m s}^{-1}$  (Panizza & Martinez-Huitle 2013) reported in literature. It is worth mentioning that in current intensity below  $I_{lim}$  no side reaction was happening, resulting in insignificant ammonia oxidation. Therefore,  $I_{lim}$  was considered as the minimum range for current intensity.

### 3.2 Organic and inorganic carbon removal

Mechanisms of electro-oxidation of each macro-pollutant could be interpreted by its kinetic model. For  $I_{app} < I_{lim}$ , operating regime was under current intensity control in which the rate of pollutant oxidation was constant (Díaz et al. 2011). In the case of our experiment, oxidation rate was always controlled by mass transfer. According to the results (showed in supplement: Table 1-S), oxidation of carbon macro-pollutants include COD, TOC, color, and TA perfectly described by the pseudo first order kinetics with  $R^2$  of 90% for all current density (Anglada et al. 2011, Bashir et al. 2013, Urtiaga et al. 2009). As illustrated in Figure 2.a, by increasing CD from 7.7 to 38.5 mA cm<sup>-2</sup>, oxidation half-life decreased rapidly, followed by gradual increase till 61.5 mA cm<sup>-2</sup>. This trend was also detected in previous studies for the treatment of refinery wastewater (Ighilahriz et al. 2013, Skban Ibrahim et al. 2014). As it shown in Figure 3, oxidation occurs in three different sections: (1) direct electric oxidation on the surface of anode (Espinoza et al. 2016), (2) OH° oxidation in the interface with formation potential of 2.8 V (3) bulk or indirect oxidation by mediators, such as HClO with  $E^\circ = 1.48$  V and H<sub>2</sub>S<sub>2</sub>O<sub>8</sub> with  $E^\circ = 2.10$  V (Espinoza et al. 2016, Panizza et al. 2001). Increase current density more than its critical value, caused side reaction of O<sub>2</sub> and Cl<sub>2</sub> production instead of hydroxyls radical on the surface of anode (Santos et al. 2006). Although it decreased dramatically the  $\eta$ , yet, additional indirect oxidation increased the constant rate of carbon oxidation. The half-life oxidation of COD, for example was between 30 to 100 min for the current density of 38.5 and 7.7 mA cm<sup>-2</sup>, respectively. As shown in Figure 3, oxidation of water molecule on the surface of BDD resulted in simultaneous production OH°, and H<sup>+</sup>. Alkalinity includes CO<sub>3</sub><sup>2-</sup> and HCO<sub>3</sub><sup>-</sup> was acted as the buffer and neutralized the excess protons; therefore, for the first hour of the reaction pH remained unchanged (the result is presented in Figure 1-S). Furthermore, reaction of alkalinity

1  
2  
3  
4 with  $\text{OH}^\circ$ ,  $\text{O}_3$ , and  $\text{H}_2\text{O}_2$  at the beginning of operation led to the production of  $\text{OH}^-$ , which even  
5  
6 raised pH in the first thirty minutes of the experiment (Ighilahriz et al. 2013, Zhou et al. 2016).

7  
8  
9 Previous studies showed that oxidation rate constant was enhanced in higher pH, since it induced  
10  
11 generation of more  $\text{OH}^\circ$  from mediator in the bulk (Alizadeh Kordkandi & Mohaghegh Motlagh  
12  
13 2017). Both reactions resulted in rapid oxidation rate with half-life of 25-64 min for the current  
14  
15 density of 38.5 and 7.7  $\text{mA cm}^{-2}$ , respectively. TOC, on the other hand, had the lowest kinetic  
16  
17 constant (between 0.14 to 0.89  $\text{h}^{-1}$ ), as the total mineralization of organic carbon to  $\text{CO}_2$  was  
18  
19 required. Finally, electro-floatation led to have complete removal hydrophobic oil and grease  
20  
21 (O&G) in very short time. Oxygen as a side reaction in anode, and hydrogen in cathode,  
22  
23 produced fine bubbles range from 15 to 60  $\mu\text{m}$  in the anode and 8-15  $\mu\text{m}$  in the cathode that  
24  
25 attached to the pollutants, floated them on the surface (Drogui et al. 2007, Santos et al. 2006). It  
26  
27 worth mentioning that rate of electro-floatation rapidly increased in higher current density; yet it  
28  
29 had insignificant effect on TOC and COD kinetic rate in our case due to small share of O&G  
30  
31 from total organic carbon (11%) (Santos et al. 2006). Complete removal of total petroleum  
32  
33 hydrocarbon in just 24 min was also reported in previous studies by CD of 30  $\text{mA cm}^{-2}$  (Rocha et  
34  
35 al. 2012, Skban Ibrahim et al. 2014).

### 3.3 Nitrogen removal

36  
37  
38 In electro-oxidation process, ammonia is only removed by reaction with  $\text{HClO}$  or  $\text{ClO}^-$  to  
39  
40 produce chloramines (Figure 3). As you can see in Table 1, decrease in concentration of chlorine  
41  
42 by 90% was result of its reaction with ammonia. As the concentration of  $\text{HClO}$  should be  
43  
44 considered in ammonia oxidation,  $\text{N}_{\text{tot}}$  and  $\text{NH}_4^+$  oxidation were fitted with second-order reaction  
45  
46 with  $\text{R}^2$  of 95% for the current density higher than 7.7  $\text{mA cm}^{-2}$ ; yet, production of  $\text{NO}_3^-$  from  
47  
48 oxidation of  $\text{NH}_4^+$ , followed zero order kinetic. As the reaction on the surface of electrode  
49  
50  
51  
52  
53  
54  
55  
56  
57  
58  
59  
60  
61  
62  
63  
64  
65

1  
2  
3  
4 followed the zero-order kinetics (Figure 2.b), it could be deduced that production of nitrate  
5  
6 mainly happened by the oxidation of ammonia on the surface of electrode. On the other hand,  
7  
8 indirect oxidation by HClO in the bulk frequently targeted  $\text{NH}_4^+$  oxidation into nitrogen gases  
9  
10 ( $\text{N}_2$ ) (Cao et al. 2016, Ighilahriz et al. 2013, Li & Liu 2009). Therefore,  $\text{N}_{\text{tot}}$  and  $\text{NH}_4^+$  was  
11  
12 followed the second-order reaction (Díaz et al. 2011). If the operating condition was not in favor  
13  
14 indirect oxidation (in acidic pH, low current density and  $\text{Cl}^-$  concentration), linear profile of  
15  
16 nitrogen oxidation (zero order kinetic) was detected (Díaz et al. 2011).  
17  
18  
19  
20

21  
22 Half-life of carbon pollutant oxidation was at least ten times faster than nitrogen pollutants half-  
23  
24 life (3 to 24 h) in different current densities. Low oxidation rates of  $\text{NH}_4^+$  and  $\text{N}_{\text{tot}}$  were also  
25  
26 reported in previous studies (Urtiaga et al. 2009).  
27  
28  
29  
30  
31

### 32 33 **3.4 Metal removal**

34  
35 Unlike ~~nitrogen~~, inorganic and organic nitrogen and carbon, metals should be reduced on the  
36  
37 cathode by electro-deposition. Metal precipitation by hydroxide ions ( $\text{OH}^-$ ) was the second  
38  
39 pathway of metal removal, especially in higher current density. According to Figure 3, Mg and  
40  
41 Ca were precipitated in the presence of  $\text{OH}^-$  produced by bicarbonate oxidation. Therefore,  
42  
43 removal efficiency more than 50% was expected for both Mg and Ca. In lower current density,  
44  
45 initial sulfur concentration rarely changed; yet in current density higher than  $23.1 \text{ mA cm}^{-2}$ ,  
46  
47 sulfate ions was transformed to  $\text{H}_2\text{S}_2\text{O}_8$  by reaction with  $\text{OH}^\circ$ , dramatically reduced average S  
48  
49 concentration from 372 to 121  $\text{mg L}^{-1}$  (Table 1). It is possible that metal cations formed a solid  
50  
51 complex with  $\text{S}_2\text{O}_8^{2-}$  ions (Dvorak et al. 1992). For the metal with no interaction with anions,  
52  
53 electro-deposition was the basic removal pathway. As respect of their positive charge, they  
54  
55 readily adsorbed on the surface of cathode and reduced to free metal. According to Figure 4,  
56  
57  
58  
59  
60  
61  
62  
63  
64  
65

1  
2  
3  
4 except Na, K, B and Si, removal efficiencies of metal were larger than 50% using different  
5  
6 current intensities. In comparison with Fe, Mg, Mn and Ca, no removal of highly reactive metal  
7  
8 such as B, Na and K was reported in literatures (da Silva et al. 2013, Rocha et al. 2012).  
9

10  
11 Silicon was mostly found in colloids and suspended solid, due to leaching of silica from the soil.  
12  
13 Although, organic matter aggregates were easily broken, decreasing the turbidity (Table 1)  
14  
15 (Santos et al. 2006), inorganic particles was basically inactive toward reduction; so, removal  
16  
17 efficiency of silicon was very low and fluctuated between 19 to 26% in different operating  
18  
19 condition (Figure 4). As the concentration of metal, alkalinity, and sulfate was decreased,  
20  
21 electrical conductivity was gradually decreased throughout the experiment (the result is  
22  
23 presented in Figure 2-S).  
24  
25  
26  
27  
28  
29  
30  
31  
32

### 33 **3.5 Process Optimization**

34  
35 Type of electrodes, current density, electrolyte addition, recycling flow rate and pH are among  
36  
37 the most important factors on the energy consumption and performance of electro-oxidation. To  
38  
39 have the highest performance, type of electrode and circulation flow rate was fixed. Moreover,  
40  
41 fixing pH was not recommended, due to its operational obstacle. Therefore, current density,  
42  
43 treatment time and electrolyte addition wasere the only variables for the optimization.  
44  
45  
46  
47

48 In order to having COD below discharge regulation ( $160 \text{ mg L}^{-1}$ ), the range of 23-38.5  $\text{mA cm}^{-2}$   
49  
50 of current density, 1-2 hours of treatment time was selected. FD model was run for eight sets of  
51  
52 experiments to figure out the following models for SEC, COD and TOC removal (Equation 6-8):  
53  
54  
55  
56  
57  
58

$$59 \text{COD RE}(\%) = 70.21 + 9.14 X_1 + 9.92 X_2 - 5.65 X_3 - 1.58 X_{12} + 5.38 X_{13}$$

60  
61  
62  
63  
64  
65

1  
2  
3  
4  $R^2= 0.996$  (6)  
5  
6  
7  
8  
9

10  $TOC RE(\%) = 53.70 + 9.33 X_1 + 15.34 X_2 - 8.27 X_3 + 3.17 X_{13} + 2.45 X_{23}$   
11

12  $R^2= 0.990$  (7)  
13  
14  
15  
16  
17

18  $SEC (kWh/kgCOD) = 100.37 + 20.86 X_1 + 19.82 X_2 - 19.22 X_3 + 7.33 X_{12} - 11.19 X_{13}$   
19  
20

21  $R^2= 0.993$  (8)  
22  
23  
24  
25  
26

27 The predicted correlation coefficients were 0.94, 0.84, 0.89, respectively, which exceeded 0.8,  
28 showed high predictability of models. Based on Pareto chart (Figure 2-S), influence of each  
29 factors and their interaction on the responses were fully described. As shown in Figure 5, and  
30 [Table 2](#) treatment time had the largest effect on COD removal efficiency. Effect of this factor on  
31 TOC removal efficiency was more pronounced. As it expected, electrolyte addition had  
32 significant effect on the energy consumption. Strangely, this factor negatively affected COD and  
33 TOC removal efficiency (Equations 6 and 7), even though it claimed that addition of electrolyte  
34 was conducive for oxidation rate (Skban Ibrahim et al. 2014). As indirect oxidation rate  
35 decreased in acidic solution, decreasing pH during the electro-oxidation process negatively affect  
36 the reaction capacity of mediator, decreasing COD and TOC removal efficiencies. It seems that  
37 electrolyte addition was also negatively affected the indirect oxidation of ammonia, as it  
38 decreased  $NH_4^+$  and  $N_{tot}$  removal efficiencies from the range of 29-39% and 12-23% to 14-29%  
39 and 9-21%, respectively. As shown in Figure 3, indirect oxidation by  $HClO$  was the main  
40 removal pathway of ammonia. This reaction was mostly determined by the concentration of  
41  
42  
43  
44  
45  
46  
47  
48  
49  
50  
51  
52  
53  
54  
55  
56  
57  
58  
59  
60  
61  
62  
63  
64  
65

1  
2  
3  
4 chloride and pH (Li &Liu 2009). By increasing the concentration of  $SO_4^{2-}$ , the rate of HClO  
5  
6 production was decreased, leading in lower ammonia oxidation. Furthermore, pH of the effluent  
7  
8 was decreased more rapidly in presence of salt. Therefore, ammonia oxidation was inhibited (Li  
9  
10 &Liu 2009).  
11

12  
13  
14 For the process optimization, CCD model was used to model the responses according to the  
15  
16 following equation (Equation 9 and 11).  
17  
18  
19  
20  
21  
22

$$23 \quad COD \text{ RE}(\%) = 70.57 + 8.42 X_1 + 10.52 X_2 + 6.34 X_3 - 1.58 X_{12} - 3.06 X_{13}$$
$$24$$
$$25 \quad R^2 = 0.957 \quad (9)$$
$$26$$
$$27$$
$$28$$
$$29$$
$$30$$

$$31 \quad TOC \text{ RE}(\%) = 55.51 + 9.51 X_1 + 15.20 X_2 + 8.34 X_3 + 1.99 X_{12} - 2.60 X_{13}$$
$$32$$
$$33 \quad R^2 = 0.954 \quad (10)$$
$$34$$
$$35$$
$$36$$
$$37$$
$$38$$

$$39 \quad SEC \text{ (kWh/kgCOD)} = 102.94 + 22.51 X_1 + 19.60 X_2 + 21.17 X_3 + 7.33 X_{12} + 9.34 X_{13}$$
$$40$$
$$41 \quad R^2 = 0.971 \quad (11)$$
$$42$$
$$43$$
$$44$$
$$45$$
$$46$$
$$47$$

48 Significance of the following models was assessed by the ANOVA test, based on 95% of the  
49  
50 confidential level. Calculated F values for equation 9 to 11 were 88, 82, and 132, respectively  
51  
52 that were superior to Fc value (predictably of model are shown in supplement: Figure 3-S). For  
53  
54 the optimization of operating condition, maximizing TOC and COD removal efficiencies, and  
55  
56 minimizing energy consumption was considered. Based on the models (result presented in  
57  
58  
59  
60  
61  
62  
63  
64  
65

1  
2  
3  
4 **Figure 4-S)** the following operating condition was required: Anode type: Nb/BDD, Cathode  
5  
6 type: Ti/Pt, current density of  $23.1 \text{ mA cm}^{-2}$ , treatment time: 120 min without addition of  
7  
8 electrolyte. For the final validation of models, three experiments run in this condition with the  
9  
10 results presented in **Table 1**. Even though COD and TOC showed high removal rate, BOD was  
11  
12 rarely decreased, as the organic carbon in the effluent had very low molecular weight with high  
13  
14 bioavailability. Low production of  $\text{NO}_3^-$  by anodic oxidation of  $\text{NH}_3$  was also detected, as the  
15  
16 most ammonia in the form of  $\text{NH}_4^+$  had lower affinity toward anode.  $\eta$  and current efficiency  
17  
18 were measured around 47.4 and 48.7%. The energy consumption required for the oxidation of  
19  
20 oily wastewater was estimated around  $102 \text{ kWh kg COD}^{-1}$  or  $86.4 \text{ kWh m}^{-3}$  that was comparable  
21  
22 with the results in the literature.  
23  
24  
25  
26  
27  
28  
29  
30  
31  
32  
33  
34  
35  
36  
37  
38  
39  
40  
41  
42  
43  
44  
45  
46  
47  
48  
49  
50  
51  
52  
53  
54  
55  
56  
57  
58  
59  
60  
61  
62  
63  
64  
65

## 4 Conclusion

Proper treatment of pollutants from oily wastewater was reached by utilization of electro-chemical oxidation process; while, physical and biological processes faced serious treatment challenges. In the anode surface, organic nitrogen and carbon could oxidized and produced  $\text{CO}_2$  and  $\text{NO}_3^-$  with zero order kinetic rate. The remaining organic and inorganic carbon was mostly targeted by hydroxyl radical with first-order kinetic rate. Indirect oxidation in bulk, especially with  $\text{HClO}$ , was responsible for  $\text{N}_{\text{tot}}$  removal with second-order reaction. Electro-floatation and electro-deposition were simultaneously occurred. Rapid removal of oil and grease was resulted from flotation by the fine hydrogen and oxygen bubbles produced in the cathode and anode, respectively. Reduction on the cathode and precipitation by sulfur and  $\text{OH}^-$  were the main removal pathways of metals.

Testing different current density, treatment time and electrolyte addition showed that the effect of the first factor was equal on COD removal efficiency and energy consumption (34.4 and 31.6%, respectively); while, the effect of last was more pronounced in energy consumption than removal efficiencies (26.8, 16.8, 13.2%, respectively). Treatment time was the most important factor on the performance of the process.

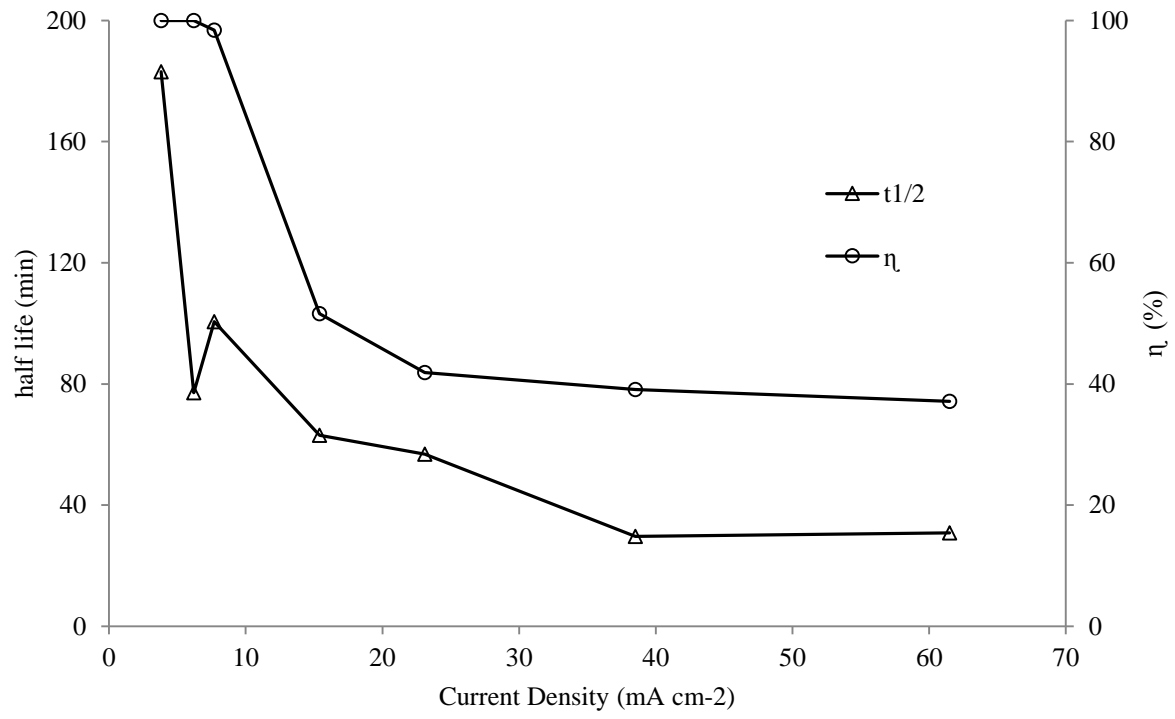
By optimizing the process, the following result was observed for current density of  $23.1 \text{ mA cm}^{-2}$  during 120 min: Removal efficiencies higher than 75% were measured for oil and grease, color, total alkalinity, COD, S,  $\text{PO}_4^{3-}$ , Al, Fe, Mn and Ca. TOC, BOD,  $\text{P}_{\text{tot}}$ , Mg, S had medium removal rates. Finally, removal efficiencies lower than 25% were detected for  $\text{N}_{\text{tot}}$ ,  $\text{NH}_4^+$ , K, and Na.

## 5 References

- Al-Shamrani AA, James A, Xiao H (2002): Destabilisation of oil–water emulsions and separation by dissolved air flotation. *Water Research* 36, 1503-1512
- Alizadeh Kordkandi S, Mohaghegh Motlagh A (2017): Optimization of peroxone reaction rate using metaheuristic approach in the dearomatization and discoloration process. *Environmental Progress & Sustainable Energy*, 1-8
- Anglada A, Urtiaga A, Ortiz I, Mantzavinos D, Diamadopoulos E (2011): Boron-doped diamond anodic treatment of landfill leachate: evaluation of operating variables and formation of oxidation by-products. *Water Res* 45, 828-38
- Bashir MJK, Aziz HA, Aziz SQ, Abu Amr SS (2013): An overview of electro-oxidation processes performance in stabilized landfill leachate treatment. *Desalination and Water Treatment* 51, 2170-2184
- Boye B, Brillas E, Marselli B, Michaud P-A, Comninellis C, Dieng MM (2004): Electrochemical decontamination of waters by advanced oxidation processes (AOPS): Case of the mineralization of 2, 4, 5-T on BDD electrode. *Bulletin of the Chemical Society of Ethiopia* 18
- Cao Z, Wen D, Chen H, Wang J (2016): Simultaneous Removal of COD and Ammonia Nitrogen Using a Novel Electro-Oxidation Reactor: A Technical and Economic Feasibility Study. *International Journal of Electrochemical Science*, 4018-4026
- Chen G (2004): Electrochemical technologies in wastewater treatment. *Separation and Purification Technology* 38, 11-41
- da Silva AJC, dos Santos EV, de Oliveira Morais CC, Martínez-Huitle CA, Castro SSL (2013): Electrochemical treatment of fresh, brine and saline produced water generated by petrochemical industry using Ti/IrO<sub>2</sub>–Ta<sub>2</sub>O<sub>5</sub> and BDD in flow reactor. *Chemical Engineering Journal* 233, 47-55
- Díaz V, Ibáñez R, Gómez P, Urtiaga AM, Ortiz I (2011): Kinetics of electro-oxidation of ammonia-N, nitrites and COD from a recirculating aquaculture saline water system using BDD anodes. *Water Research* 45, 125-134
- Ding J, Li W, Zhao Q-L, Wang K, Zheng Z, Gao Y-Z (2015): Electroreduction of nitrate in water: Role of cathode and cell configuration. *Chemical Engineering Journal* 271, 252-259
- Drogui P, Blais J-F, Mercier G (2007): Review of electrochemical technologies for environmental applications. *Recent patents on engineering* 1, 257-272
- Dvorak DH, Hedin RS, Edenborn HM, McIntire PE (1992): Treatment of metal-contaminated water using bacterial sulfate reduction: Results from pilot-scale reactors. *Biotechnology and bioengineering* 40, 609-616
- Espinoza JDG, Drogui P, Zolfaghari M, Dirany A, Ledesma MTO, Gortáres-Moroyoqui P, Buelna G (2016): Performance of electrochemical oxidation process for removal of di (2-ethylhexyl) phthalate. *Environmental Science and Pollution Research* 23, 12164–12173
- Ighilahriz K, Ahmed MT, Djelal H, Maachi R (2013): Electrocoagulation and electro-oxidation treatment for the leachate of oil-drilling mud. *Desalination and Water Treatment* 52, 5833-5839
- Körbahti BK, Artut K (2010): Electrochemical oil/water demulsification and purification of bilge water using Pt/Ir electrodes. *Desalination* 258, 219-228

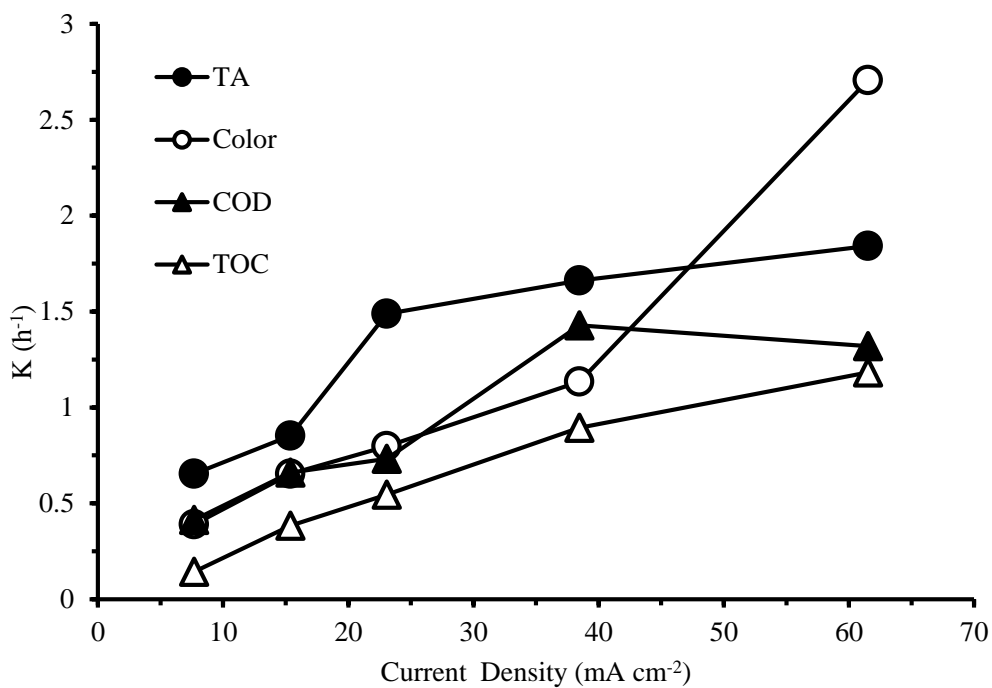
- 1  
2  
3  
4 Li L, Liu Y (2009): Ammonia removal in electrochemical oxidation: Mechanism and pseudo-kinetics.  
5 Journal of hazardous materials 161, 1010-1016  
6
- 7 Martínez-Huitle CA, Brillas E (2008): Electrochemical alternatives for drinking water disinfection.  
8 *Angewandte Chemie International Edition* 47, 1998-2005  
9
- 10 Panizza M, Michaud P, Cerisola G, Comninellis C (2001): Anodic oxidation of 2-naphthol at boron-  
11 doped diamond electrodes. *Journal of Electroanalytical Chemistry* 507, 206-214  
12
- 13 Panizza M, Martínez-Huitle CA (2013): Role of electrode materials for the anodic oxidation of a real  
14 landfill leachate--comparison between Ti-Ru-Sn ternary oxide, PbO(2) and boron-doped diamond  
15 anode. *Chemosphere* 90, 1455-60  
16
- 17 Rocha JHB, Gomes MMS, Fernandes NS, da Silva DR, Martínez-Huitle CA (2012): Application of  
18 electrochemical oxidation as alternative treatment of produced water generated by Brazilian  
19 petrochemical industry. *Fuel processing technology* 96, 80-87  
20
- 21 Santos MR, Goulart MO, Tonholo J, Zanta CL (2006): The application of electrochemical technology to  
22 the remediation of oily wastewater. *Chemosphere* 64, 393-399  
23
- 24 Skban Ibrahim D, Seethala Devi P, Veerababhu C, Balasubramanian N (2014): Treatment of Petroleum  
25 Effluent Using a Tubular Electrochemical Reactor. *Petroleum Science and Technology* 32, 1932-  
26 1939  
27
- 28 Tazari F, Rahaie M, Zarmi AH, Jalili H, Yazdian F, Kordkandi SA (2017): A Systematic Comparison of  
29 Biosurfactant Effects on Physicochemical Properties and Growth Rates of *P. aeruginosa* MM1011  
30 and TMU56: A Bioremediation Perspective. *Bioprocess Engineering* 1, 14-20  
31
- 32 Urtiaga A, Rueda A, Anglada A, Ortiz I (2009): Integrated treatment of landfill leachates including  
33 electrooxidation at pilot plant scale. *Journal of hazardous materials* 166, 1530-4  
34
- 35 Yavuz Y, Koparal AS, Ögütveren ÜB (2010): Treatment of petroleum refinery wastewater by  
36 electrochemical methods. *Desalination* 258, 201-205  
37
- 38 Yu L, Han M, He F (2017): A review of treating oily wastewater. *Arabian Journal of Chemistry* 10, 1913-  
39 1922  
40
- 41 Yu Z-m, Jian W, WEI Q-p, Meng L-c, Hao S-m, Fen L (2013): Preparation, characterization and  
42 electrochemical properties of boron-doped diamond films on Nb substrates. *Transactions of*  
43 *Nonferrous Metals Society of China* 23, 1334-1341  
44
- 45 Zhou B, Yu Z, Wei Q, Long H, Xie Y, Wang Y (2016): Electrochemical oxidation of biological  
46 pretreated and membrane separated landfill leachate concentrates on boron doped diamond anode.  
47 *Applied Surface Science* 377, 406-415  
48
- 49 Zolfaghari M, Jardak K, Drogui P, Brar SK, Buelna G, Dubé R (2016): Landfill leachate treatment by  
50 sequential membrane bioreactor and electro-oxidation processes. *Journal of environmental*  
51 *management* 184, 318-326  
52  
53  
54  
55  
56  
57  
58  
59  
60  
61  
62  
63  
64  
65

Figure 1

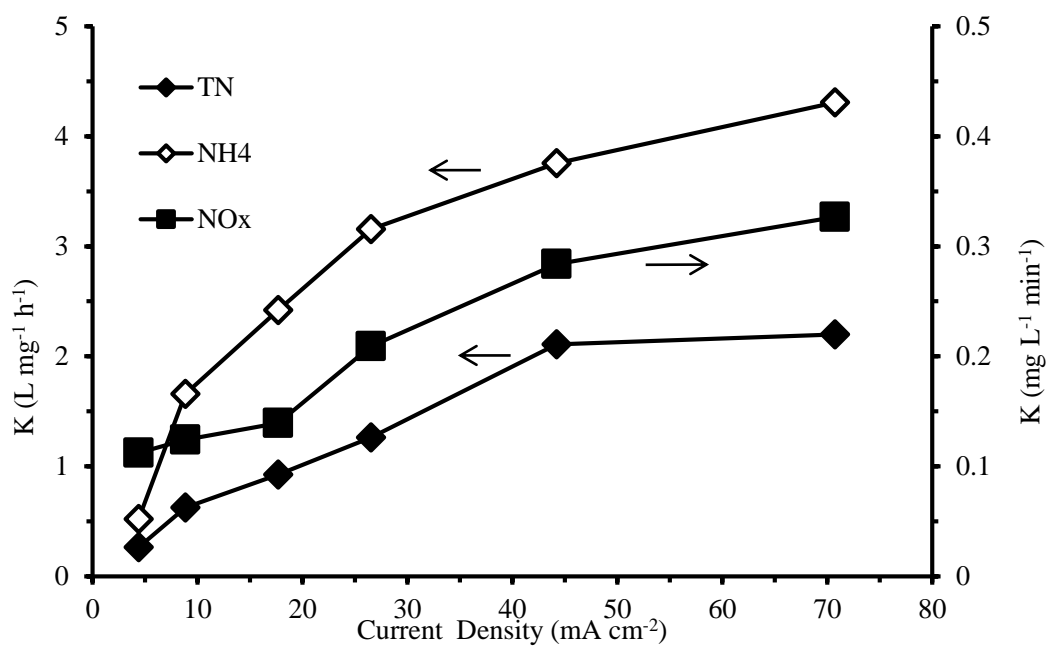


**Figure 1.** The apparent COD oxidation half-life and instantons current efficiency in different current densities.

Figure 2



(a)



(b)

**Figure 2.** The apparent reaction rate constant of (a) pseudo-first order kinetic for COD, TOC, TA, and color (b) pseudo-second and zero order kinetic for  $N_{\text{tot}}$ ,  $\text{NH}_4^+$ ,  $\text{NO}_3^-$  in different current densities.

Figure 3

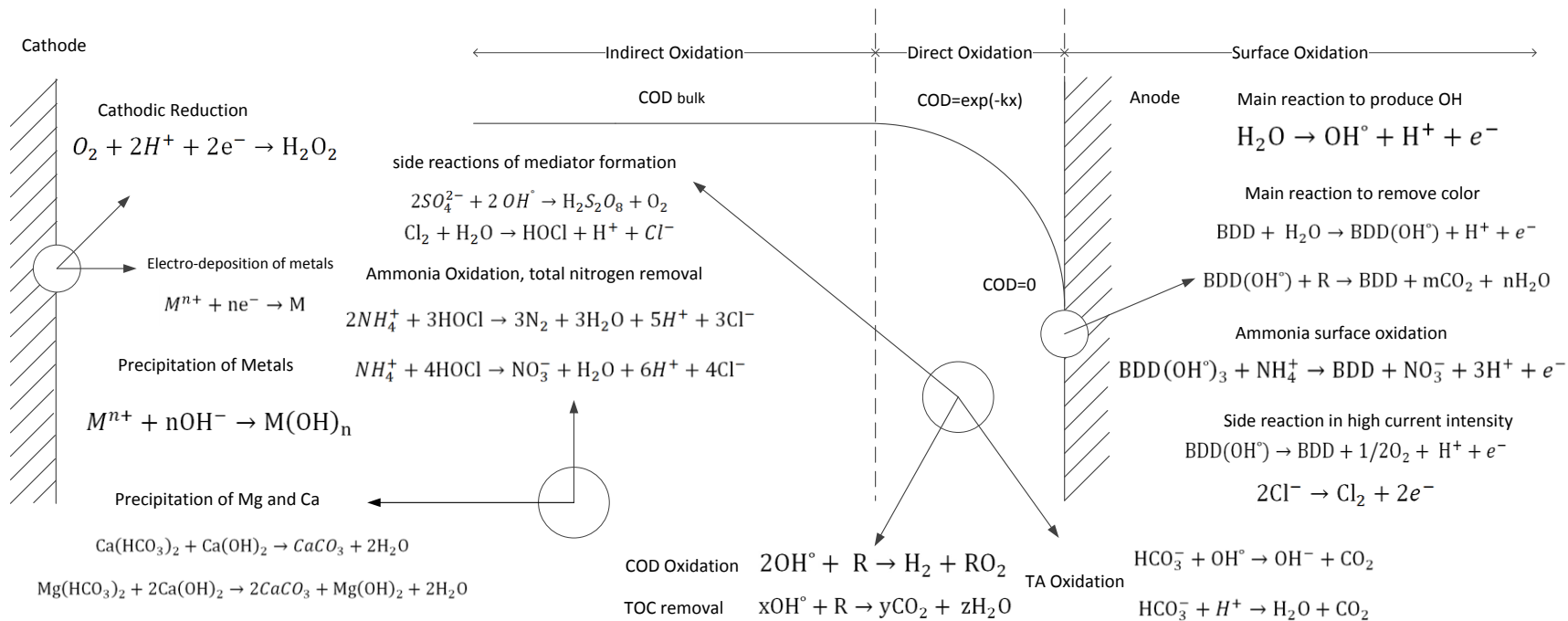
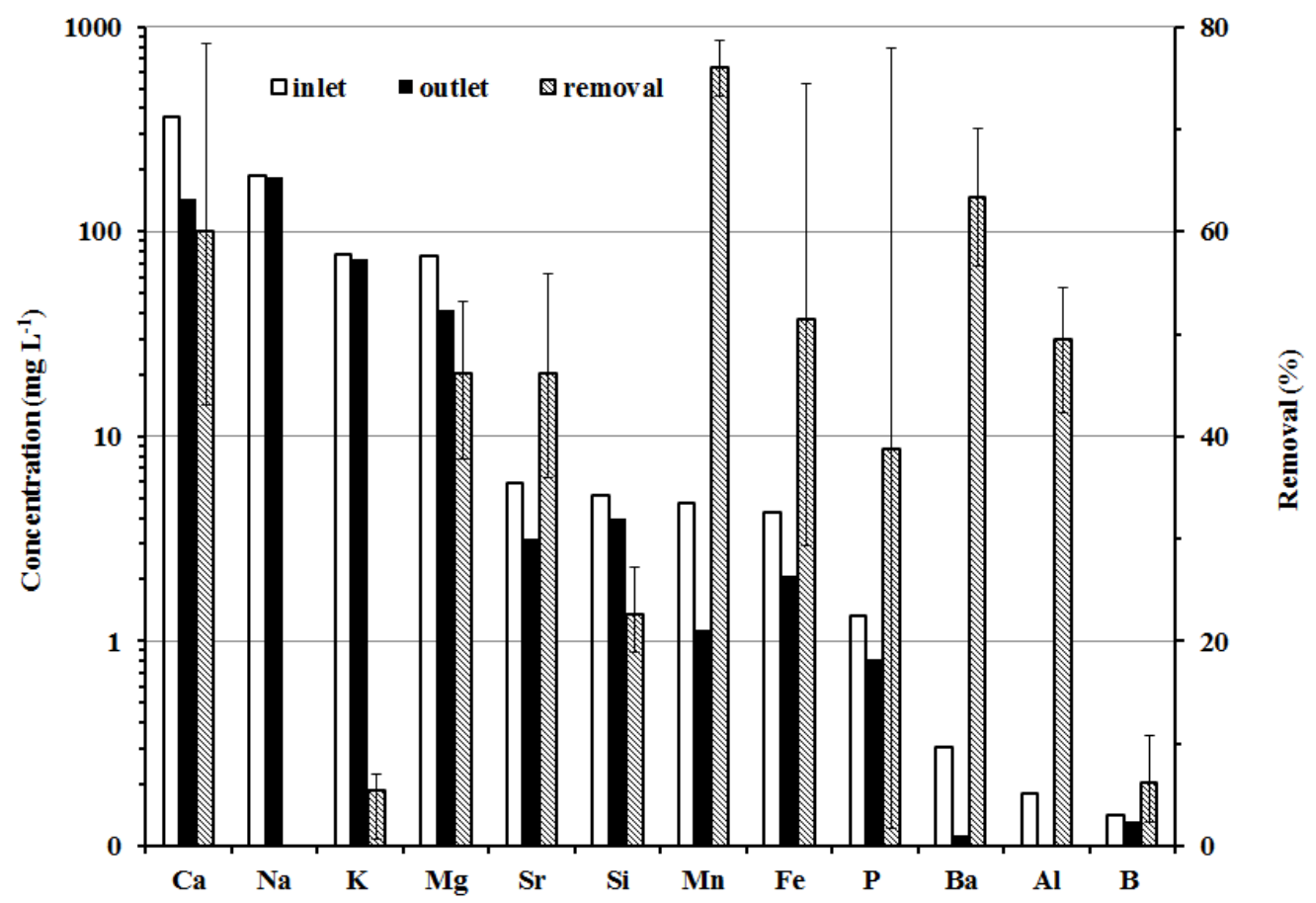


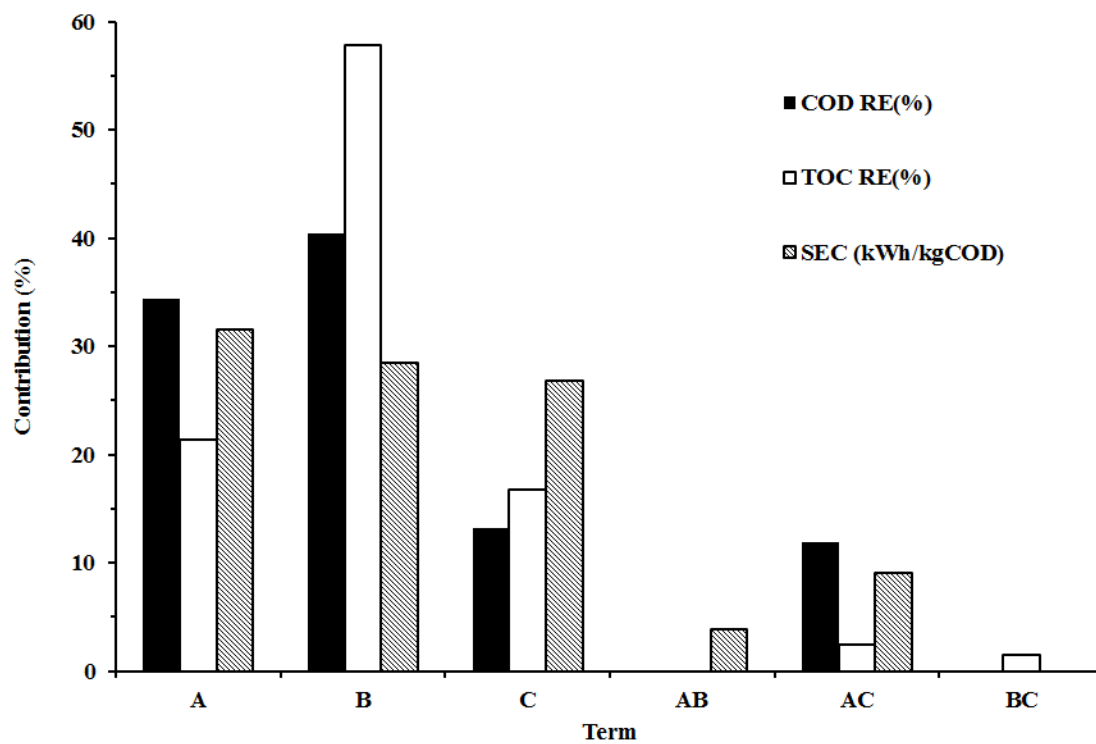
Figure 3. Removal mechanism of all macro-pollutants by electro-oxidation process.

Figure 4



**Figure 4.** Average removal efficiency, influent and effluent concentration of metal cations in different treatment time (1-3 h) and current density (3.8-61.5 mA cm<sup>-2</sup>).

Figure 5



**Figure 5.** Contribution of all factor (A: Current density, B: Treatment time, C: Electrolyte addition) on the responses.

**Table 1.** Characterization of oily wastewater and the performance of electro-oxidation in the optimum operating condition (CD = 23.1 mA cm<sup>-2</sup>, t = 120 min, T = 25°C).

Parameters (unit)	Influent	Effluent	Removal (%)
TOC (mg C L <sup>-1</sup> )	378 ± 12	120 ± 14	68 ± 2
O&G (mg C L <sup>-1</sup> )	43.7 ± 5	ND	100
COD (mg O <sub>2</sub> L <sup>-1</sup> )	1,160 ± 215	154 ± 25	85 ± 2
BOD (mg O <sub>2</sub> L <sup>-1</sup> )	98 ± 15	43 ± 12	56 ± 3
N <sub>tot</sub> (mg N L <sup>-1</sup> )	76 ± 2	63 ± 1	18 ± 3
NH <sub>4</sub> (mg N L <sup>-1</sup> )	54 ± 1	38 ± 3	31 ± 4
NO <sub>3</sub> (mg N L <sup>-1</sup> )	0.4 ± 0.2	21 ± 2	-
PO <sub>4</sub> (mg P L <sup>-1</sup> )	0.5 ± 0.2	0.1 ± 0.2	80 ± 10
P <sub>tot</sub> (mg P L <sup>-1</sup> )	1.3 ± 0.2	0.2 ± 0.2	75 ± 20
TA (mg CaCO <sub>3</sub> L <sup>-1</sup> )	695 ± 15	58 ± 5	92 ± 2
Color (TCU)	303 ± 24	23 ± 3	88 ± 1
EC (ms cm <sup>-1</sup> )	-	2.52 ± 0.24	-
pH	7.12 ± 0.13	7.31	-
TS (mg L <sup>-1</sup> )	2,750 ± 110	-	-
TVS (mg L <sup>-1</sup> )	835 ± 20	290 ± 50	65 ± 4
Al (mg L <sup>-1</sup> )	0.2 ± 0.1	0.09 ± 0.07	48 ± 24
Ca (mg L <sup>-1</sup> )	362 ± 1	122 ± 10	66 ± 3
Fe (mg L <sup>-1</sup> )	4.3 ± 0.1	1.2 ± 0.3	71 ± 12
K (mg L <sup>-1</sup> )	78 ± 1	72 ± 1	7 ± 1
Mg (mg L <sup>-1</sup> )	77 ± 1	45 ± 2	41 ± 2
Mn (mg L <sup>-1</sup> )	4.8 ± 0.1	1.0 ± 0.1	78 ± 4
S (mg L <sup>-1</sup> )	97 ± 1	24 ± 5	75 ± 5
Cl (mg L <sup>-1</sup> )	147 ± 1	16 ± 2	89 ± 11
Si (mg L <sup>-1</sup> )	5.1 ± 0.1	4.2 ± 0.6	19 ± 14
Sr (mg L <sup>-1</sup> )	5.9 ± 0.1	2.9 ± 1.2	51 ± 21
B (mg L <sup>-1</sup> )	0.14 ± 0.01	0.13 ± 0.01	-

TA : total alkalinity, TS : total solid, TVS : total volatile solid

**Table 2.** Initial conditions and responses of the electro-oxidation processes for all sets of experiments, including factorial and central composite design.

Run	Factors				Responses		
	Current density (mA cm <sup>-2</sup> )	Time (min)	Electrolyte addition	Voltage (V)	SEC (kWh kg COD <sup>-1</sup> )	COD removal efficiency (%)	TOC removal efficiency (%)
1	30.8	90	No	17.0	128.5	79.2	68.0
2	41.5	90	Yes	14.2	109.4	74.7	63.5
3	23.1	120	Yes	11.7	82.2	60.5	47.9
4	23.1	60	Yes	11.3	60.8	39.5	18.0
5	20.0	90	No	13.4	76.8	67.5	51.1
6	23.1	120	No	14.4	101.8	84.6	68.3
7	30.8	90	Yes	12.5	81.2	65.5	49.5
8	30.8	47.6	Yes	13.1	62.0	47.5	18.0
9	38.5	60	No	17.0	120.4	70.4	54.8
10	30.8	132.4	Yes	13.2	101.6	81.3	70.9
11	38.5	60.0	Yes	13.7	67.8	71.7	37.3
12	38.5	120	Yes	13.9	113.9	86.5	78.6
13	30.8	90	No	17.0	131.1	77.6	66.4
14	30.8	90	No	17.0	131.6	77.3	64.0
15	30.8	90	Yes	12.2	80.4	64.6	51.3
16	30.8	90	No	17.0	125.7	78.5	65.1
17	23.1	60	No	14.6	73.3	59.6	43.4
18	30.8	90	Yes	11.7	79.0	63.0	55.0
19	20.0	90	Yes	11.5	62.2	50.8	32.3
20	38.5	120	No	16.3	182.9	88.9	81.5
21	30.8	90	Yes	11.7	72.5	68.6	44.7
22	30.8	90	Yes	12.9	90.2	60.8	48.9
23	30.8	90	No	12.9	126.8	80.2	66.7
24	30.8	47.6	No	16.9	89.2	59.9	47.1
25	30.8	132.4	No	16.1	159.2	89.0	81.2
26	41.5	90	No	17.9	166.3	87.2	72.8